Volume 1 | Number 1 | Jan 2013 | Pages 1–100

Journal of
Materials Chemistry A

Materials for energy and sustainability
www.rsc.org/materialsA

ROYAL SOCIETY OF CHEMISTRY

www.rsc.org/materialsA

Journal of Materials Chemistry A

ARTICLE

Amino-functionalized Ordered Mesoporous Carbon for the Separation of Toxic Microcystin-LR

Wei Teng,[ab] Zhangxiong Wu,[c] Jianwei Fan,[a] Wei-xian Zhang*[a] and Dongyuan Zhao*[b]

Amino-functionalized ordered mesoporous carbon materials with high surface areas are fabricated from bimodal mesoporous carbons as the matrix and functionized with a three-step chemical modification of oxidation, acylation and amidation. Mesostructural regularity, textural evolution, property and density of the surface functional groups are characterized. The obtained amino-functionalized mesoporous carbon possesses an ordered mesostructure, a high surface area (1,063 m^2/g), a large pore volume (0.7 cm^3/g) and bimodal mesopores (2.3 and 4.8 nm). More importantly, the surface is positively charged under neutral pH. This type of nanomaterials is designed specially for sorption and separation of negatively charged large molecules due to the synergic advantages of positively charged amino groups, high surface area, and interconnected large mesopores. Batch and column experiments demonstrate its outstanding adsorption capability (580 and 334 mg/g respectively) for the removal of Microcystin-LR (M_W = 995), much better than conventional activated carbon (<64 mg/g). Properties such as porosity as well as density of the amino groups (2.73 – 3.84 mmol/g) can be further fine-tuned by adjusting the oxidation procedure. Furthermore, this material can be effectively regenerated by methanol.

Introduction

Ordered mesoporous carbon materials have long been recognized as a type of promising nanomaterials for applications in water treatment, air purification, catalysis and energy storage because of their exceptional properties such as high surface area, large pore volume, uniform and adjustable mesostructure and pore size, good chemical and thermal stability.[1-4] Recently, with the development of new synthetic techniques, mesoporous carbon materials can be more easily synthesized and manipulated.[5, 6] This offers new opportunities for environmental applications with increased availability and reduced costs. Nonetheless, the relatively inert and hydrophobic character presents a technical barrier, especially for adsorption and separation of contaminants in polar solvents such as water. Therefore, surface modification or functionalization of mesoporous carbon materials with targeted functional groups is the key toward expanding their environmental applications.

A variety of functional groups can be attached to the surface of mesoporous carbons to endow them with amazing properties,[7-9] for example, surface oxidation and activation,[10, 11] halogenation,[12] sulfonation[13] and so on. Anchoring amino groups onto carbon-based materials has attracted growing attentions because of their high reactivity, positively charged character in water, and strong affinity to some chemicals, such as noble metal, polymers, negatively charged molecules etc.[14, 15] A large number of studies have already been published on carbon-based materials including activated carbon,[16] carbon nanotube,[17-19] and graphene[20-22] functionalized with amino groups for applications in catalysis, electrochemistry and biological systems. In general, introduction of amino groups to ordered mesoporous carbons can enhance the capability of materials for sorption of negatively charged organic pollutants.

A convenient route to graft amino groups upon pristine carbon surface is to generate carboxyl groups by oxidation with concentrated nitric acid, followed with the acylation-amidation chemistry to attach amino groups. Introduction of carboxylic groups by oxidation is the most frequently used approach because carboxylic groups can easily form on carbon surface using oxidation agents and further reactions with other functional groups. However, compared with other carbon-based materials, mesoporous carbon possesses regular mesostructure and high porosity, which might be affected and damaged under strong oxidation conditions.[23, 24] Acidic ammonium persulfate [(NH$_4$)$_2$S$_2$O$_8$, APS] solution, a relatively mild oxidant is often used. It can efficiently introduce carboxylic groups to carbon surfaces while maintaining the ordered mesostructure,[25] thus yielding amino-functionalized mesoporous carbon materials with high surface area and large interconnected mesopores.

Microcystin-LR (MC-LR) is a common type of monocyclic heptapeptides produced from cyanobacteria as blue algae

[a.] College of Environmental Science and Engineering, State Key Laboratory for Pollution Control, Tongji University, Shanghai, China 200092. E-mail: zhangwx@tongji.edu.cn. Tel: +86-21-65985885.
[b.] Department of Chemistry, Shanghai Key Laboratory of Molecular Catalysis and Innovative Materials, and Advanced Materials Laboratory, Fudan University, Shanghai, China 200433. E-mail: dyzhao@fudan.edu.cn. Fax: +86-21-51630307; Tel: +86-21-51630205.
[c.] College of Chemistry, Chemical Engineering and Material Science, Soochow University, Suzhou City, Jiangsu, China 215123.

blooms (SI Figure S1).[26-28] It is very toxic to animals and human beings due to the acute and irreversible liver damages.[29, 30] However, its stable and special cyclic structure as well as large molecular size of 1.9 x 1.1 x 1.5 nm makes it difficult to be removed from water by conventional techniques such as activated carbon sorption, coagulation and filtration.[26, 31] We have studied the adsorption behaviors of different mesoporous carbon towards MC-LR.[32] A bimodal mesoporous carbon was found to exhibit relatively good adsorption capacity, but its inert surface presents an obstacle for preferable performance in water filtration. In another work about MC-LR adsorption on mesoporous silica,[33] quaternary ammonium functionalized mesoporous silica improved the adsorption capacity from 50 to 95% at pH ~4. However, the surface area of mesoporous silica was substantially less than mesoporous carbon, leading to much lower adsorption capacity. Considering that MC-LR is negatively charged, it is expected that surface amino functionalization can further improve the adsorption ability because of electrostatic attractions. Unfortunately, little has been published on the preparation of amino-functionalized mesoporous carbon materials via chemical modification, and subsequently the corresponding evolution of structural, textural, surface chemical properties and potential for the MC-LR removal are unknown.

In this paper, we have developed synthetic methods for the preparation of amino-terminated mesoporous carbon (denoted as MC-NH$_2$) with a high surface area (1,063 m^2/g) and a well-ordered mesostructure by employing post chemical modification. The modification is achieved by three steps, namely, wet oxidation to generate carboxyl group by acidic APS, reaction with thionyl chloride (SOCl$_2$), and formation of amides with amine through amidation chemistry. The functionalization can be precisely controlled by tuning the oxidation time in oxidation and ethylenediamine (EDA) addition in amidation. The density of incorporated amino groups can be increased to 3.84 mmol/g by such modifications. The corresponding changes in mesostructure, texture, surface chemistry, and surface charges are characterized in details. Finally, the functionalized mesoporous carbon is evaluated as a sorbent for the removal of toxic MC-LR from water. Batch and column adsorption experiments are conducted to compare the performance of pristine and other functionalized mesoporous carbon materials and the commercial powder activated carbon. Influence of solution pH and regeneration of amino functionalized sorbent are also investigated.

Experimental

Chemicals

Triblock copolymer poly(ethylene oxide)-b-poly(propylene oxide)-b-poly(ethylene oxide) Pluronic F127 (M_w = 12 600, EO$_{106}$PO$_{70}$EO$_{106}$) was purchased from Acros Corp. Tetraethyl orthosilicate (TEOS), phenol, formaldehyde solution (37 wt. %), hydrochloric acid, ammonium persulfate [(NH$_4$)$_2$S$_2$O$_8$, APS], sulfuric acid (H$_2$SO$_4$), ethanol, thionyl chloride (SOCl$_2$), dimethylformamide (DMF) and ethylenediamine (EDA) were

obtained from Shanghai Chemical Corp. Commercial powder activated carbon (PAC) was supplied by the Xinzhuang Activated Carbon Company of Shanghai. Microcystin-LR (MC-LR, purity > 95%) was provided by the Express Technology Co., Ltd. Trifluoroacetic acid (TFA, 99% HPLC grade) and methanol (HPLC grade) were purchased from Merck Corp. Deionized water with a resistance of > 18.2 MΩ cm^{-1} was obtained by passing tap water through a Milli-Q system. All chemicals were used as received without further treatment.

Synthesis of Amino-functionalized Ordered Mesoporous Carbon

Synthesis of the amino-functionalized ordered mesoporous carbon materials was achieved by chemical modification on a bimodal mesoporous carbon (denoted as MC), involving generation of carboxyl groups introduced by surface wet oxidation, and linkage to amines through reaction of acylation-amidation chemistry (SI Scheme S1). The ordered bimodal mesoporous carbon matrix was prepared following the approach reported by Liu et al.[2] It was a pure carbon obtained from a silica-carbon composite carbonized at 900°C and followed by silica removal. The composite could be obtained from a tri-constituent co-assembly process of silica oligomer precursors, phenolic resols, and Pluronic F127 in the initial ethanolic solution (SI Scheme S1a, b). For the chemical modification, typically, 50 mg of the pristine MC material was treated with a 1.0 M of APS solution (in 2 M H$_2$SO$_4$) at 60°C for 4 – 16 h to oxidize the carbon surface. The carboxylic solids (denoted as MC-COOH, SI Scheme S1c) were collected after filtration, washed and dried at 60°C overnight. Then, 40 mg of MC-COOH sample was refluxed in 10 mL of SOCl$_2$ and 1 mL of DMF mixed solution at 60°C for 24 h with continuous stirring to form an acyl-chloride derivative (denoted as MC-COCl, SI Scheme S1d). After washing with DMF, the obtained powder was dried again at 60°C overnight. Finally, 30 mg of resulting MC-COCl powder was added into a solution mixed with 4 – 8 μL of EDA and 5 mL of DMF, stirring at 60°C for 24 h under reflux. After washing and drying, the end product mesoporous carbons functionalized with amino groups (denoted as MC-NH$_2$, SI Scheme S1e) were obtained. The density of the amino groups attached onto the carbon matrix was controlled by two steps, including different durations in carboxylation and various amounts of EDA in amidation. The final functionalized samples are denoted as MC-NH$_2$-x-y, where x stands for the treatment time of carboxylation (h) and y for the added amount of EDA (μL), respectively.

Batch and Column Adsorption of Microcystin-LR

Batch adsorption of MC-LR on mesoporous carbon materials with different properties and PAC were carried out as follows. About 0.2 mg of carbon sorbents were dispersed in 20 mL of deionized water with an ultrasound treatment for 30 s to obtain a homogeneous suspension in a test tube. The stock solution of MC-LR was added in to reach an initial concentration of 2 mg/L. Then, the tube was sealed and shaken at 200 rpm in a thermo-stated rotary shaker at 25°C. After 4 h, 0.5 mL of the

mixture was taken out, filtered through a filter (cellulose acetate membrane) to remove the solid sorbent, and then the remaining concentration of MC-LR was determined by high performance liquid chromatography (HPLC). Adsorption kinetic experiments were performed in the same conditions as above. The MC-LR concentrations were measured at preset intervals (from 1 to 240 min). The adsorption isotherms of pristine MC and amino-functionalized MC-NH$_2$ samples were conducted in a series of initial concentrations from 0.5 to 8 mg/L for 4 h (equilibrium has reached) and the other conditions were the same as above. The pH-dependent adsorption experiments were also carried out in the same conditions and the pH values were adjusted by using a 0.1 M HCl or NaOH solution.

To evaluate the column adsorption performance, the pristine mesoporous carbon MC and amino functionalized MC-NH$_2$ powders were grinded and sieved between 500 to 700 mesh, and then packed tightly (~ 5.0 mg) to assemble a column with a diameter of 4.5 mm and a length of ~ 1.9 mm. After a buffer run with deionized water for half an hour, MC-LR feed solution (10 mg/L) was continuously pumped through the column with a constant flow rate of 0.25 mL/min at room temperature. The effluent solution was consecutively collected every 10 min and the corresponding MC-LR concentrations were measured by HPLC. Based on the detected data and calculation, the breakthrough curves and the corresponding adsorption capacities of MC-LR at 10 % breakthrough were obtained. (Details about adsorption calculation and modelling are provided in the SI.)

After one adsorption circle, methanol and deionized water were successively pumped through the column at the same flow rate to elute the adsorbed MC-LR and the residual methanol for regeneration of the mesoporous carbon filters in the column.

Characterization and measurements

Small-angle X-ray scattering (SAXS) patterns were recorded with a Nanostar U small-angle X-ray scattering system (Bruker) with a Cu Kα radiation at 40 kV and 35 mA. Transmission electron microscopy (TEM) images were taken by a JEOL JEM 2011 or a JEM 2100F microscope operated at 200 kV. Samples for TEM measurements were dispersed in ethanol and dropped onto holey carbon films supported on a Cu or micro grid. High resolution scanning electron microscopy (HRSEM) images were obtained from a Hitachi S-4800 ultrahigh resolution SEM operating at 1 kV. Nitrogen adsorption/desorption isotherms were determined with a Micromeritics Tristar 3020 analyzer at 77 K. Before the measurements, samples were degassed in vacuum at 120°C for at least 8 h. The BET method was used to calculate the surface areas (S_{BET}) by using the adsorption data at p/p_0 of 0.02 − 0.2. The total pore volume (V_t) was estimated from the adsorbed amount at p/p_0 of 0.995. The pore size distributions were derived from the adsorption branches of isotherms by using the BJH model. Fourier transform infrared (FTIR) spectra were measured on a Shimadzu IRPrestige-21 Fourier spectrophotometer from 4000 to 400 cm^{-1}. The samples were ground with solid KBr (1: 100) and then the mixture was pressed into pellet for scanning at room temperature. X-ray

photoelectron spectroscopy (XPS) was measured by a Perkin Elmer PHI5000C spectroscope with a Mg Kα line as the excitation source. The element contents of C, N, H in the samples were measured using a Vario EL III element analyzer in CHN mode. The contents of organic groups were converted in accordance with the amount of elements. Thermogravimetric (TG) analysis was carried out on a Mettler Toledo TGA/DSC 1 thermogravimetric analyzer from 40 − 900°C (10°C/min of heating rate) under N$_2$ (20 mL/min). The Zeta-potential was recorded by using a ZEN 3600 Instrument (Malvern). The samples were dispersed in 10 mL of deionized water with ultrasound for 0.5 min with the same concentration as that in adsorption tests. 0.1 M NaCl was added to maintain a high background-electrolyte concentration. Different pH values were adjusted by 0.1 M NaOH or HCl and determined by using a PHS-25 digital pH meter. Analysis of MC-LR was performed on HPLC (LC-10AT, Shimadzu) with an ultraviolet (UV) detector (Model 2478) and a C18 column (Shim-pack VP-ODS, 4.6 x 150 mm, i.d. 5 mm). The mobile phase was a mixture of methanol-water (60 : 40) containing 0.1 % of TFA (v/v) with a 0.8 mL/min at 40°C. The typical detection was carried out at 238 nm with the injection volume of 50 μL.

Results and discussion

Structural and Textural Properties of Mesoporous Carbon Materials

The structural evolutions before and after each modification procedure are observed by the transmission electron microscopy (TEM). TEM images (Figure 1a, b) show the classical stripe-like and hexagonally arranged 2-D hexagonal mesostructure in large domains viewed from the [110] and [001] directions in the pristine mesoporous carbon MC. Generally, after the modifications, all the functionalized mesoporous carbon samples still retain their original 2D hexagonal mesostructure. More specifically, after the acidic APS treatment for 4 h, the mesoporous carbon MC-COOH-1 shows a marginal change on its framework (Figure 1c). The outer carbon layers on the surface are etched to some extent. Prolonged the acidic APS treatment to 16 h, the sample MC-COOH-2 exhibits some small "holes" or "cavities" across the frameworks (Figure 1d), indicating that part of the carbon layers are removed from the carbon frameworks and then dissolved gradually. But it still preserves an ordered arrangement as a whole. During the treatment of acylation and amidation, structures of the obtained mesoporous carbon samples are retained (Figure 1e, f). However, for the sample MC-NH$_2$-1-b treated with excess EDA, it shows a slightly obscured carbon framework from the TEM images (Figure 1g, h). It can be attributed to the fact that more organic groups are generated in or outside the mesochannels. HESEM images exhibit ordered mesostructures in large domains with fully open pore channels on the surfaces for the pristine and amino-functionalized mesoporous carbon materials (SI Figure S2). Meanwhile, amino-functionalized mesoporous carbon displays

a slightly declining order and obscured surface which is caused by the functionalized groups, in keeping with the TEM results.
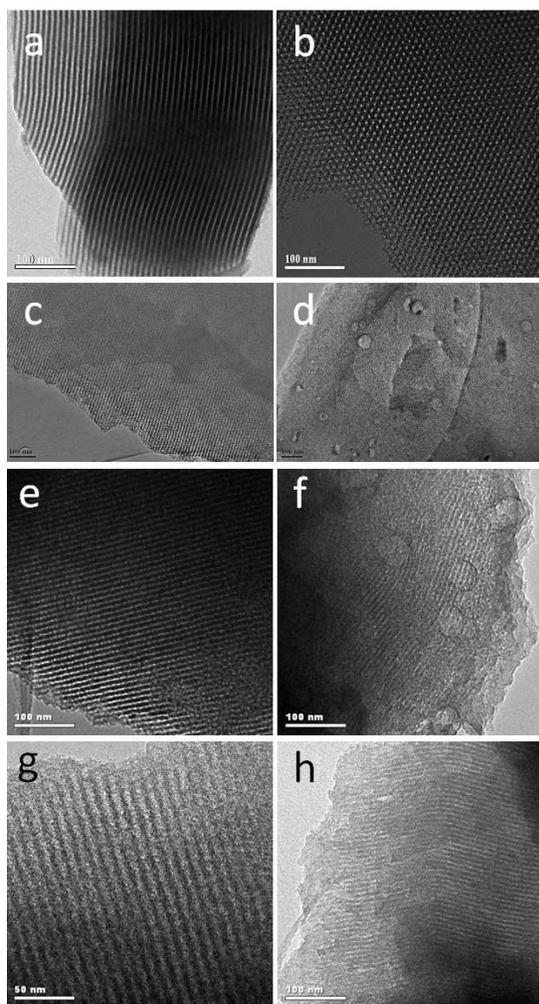
Fig. 1 TEM images of pristine ordered mesoporous carbon MC along the [10] (a) and [01] (b) directions and different functionalized mesoporous carbon samples after treatment of oxidation and acylation-amidation MC-COOH-1 (c), MC-COOH-2 (d), MC-NH$_2$-1-a (e), MC-NH$_2$-2-b (f) and MC-NH$_2$-1-b (g, h), where 1 and 2 stand for the oxidation time of 4 and 16 h, and a, b for the added amount of the EDA with 4 and 8 μL, respectively.

Small-angle X-ray scattering (SAXS) pattern of the pristine mesoporous carbon sample shows three well-resolved scattering peaks assigned to the 10, 11 and 21 reflections (SI Figure S3a), indicating a highly ordered hexagonal mesostructure (space group *p6m*), in accordance with the TEM results. After being treated with acidic APS, SOCl$_2$ and EDA in sequence, the ordered mesostructure is retained for all the resultant materials (SI Figure S3b-g). Specifically, after the first treatment of surface oxidation for 4 h, the mesoporous carbon MC-COOH-1 shows broad and less-resolved SAXS peaks. Meanwhile, the scattering peaks (e.g. the 10 reflection) shift to larger *q* values with decrease of the cell parameter. It suggests slight deterioration of mesostructural regularity and generation of functionalized groups under such acidic oxidative condition

(SI Figure S3b). After increasing the treated time to 16 h, a weaker scattering peak is observed in the sample MC-COOH-2 (SI Figure S3e), implying that the mesostructure regularity is gradually degenerated by surface oxidation and/or more oxygen containing groups are anchored onto the mesopore surface, thus reducing the X-ray contrast.
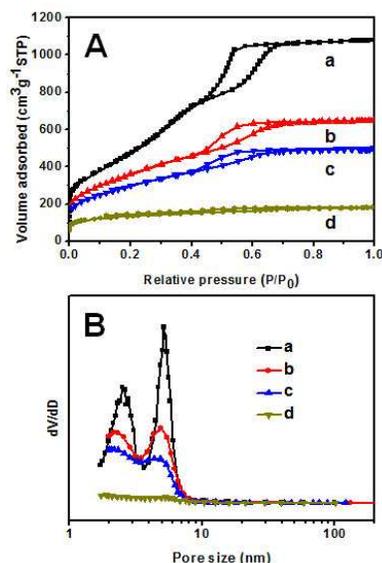
Fig. 2 Nitrogen sorption isotherms (A) and the corresponding pore size distribution curves (B) of pristine mesoporous carbon (a), functionalized mesoporous carbon samples after treatment of oxidation and acylation-amidation MC-COOH-1 (b), MC-NH2-1-a (c) and MC-NH2-2-b (d), where 1 and 2 stand for the oxidation time of 4 and 16 h, and a, b for the added amount of the EDA with 4 and 8 μL, respectively.

Nitrogen adsorption/desorption isotherms of the pristine and functionalized mesoporous carbon materials show representative type-IV curves with two condensation steps in the mesopore range (Figure 2). The pristine mesoporous carbon possesses a high surface area of 1,680 m^2/g and a large pore volume of 1.67 cm^3/g with two uniform mesopore size distributions centered at 2.8 and 5.5 nm (Table 1), which are originated from the interconnected bimodal mesopores formed by etching of surfactant F127 and the silica component. However, the surface area, pore volume and pore sizes decrease gradually after the modification procedures. The acidic APS treated (4 h) sample MC-COOH-1 shows a decreased surface area of 1,290 m^2/g, a pore volume of 0.96 cm^3/g, and mesopore sizes of 2.4 and 4.9 nm, suggesting that the oxygen-containing groups may be located on the surface of mesopores to occupy pore spaces. Moreover, the degradation effects on the frameworks caused by surface carbon layer etching are limited but evident. The carboxylic mesoporous carbon is further treated with thionyl chloride and EDA to form amide-terminated MC-NH$_2$. The surface area, pore volume and pore diameters of the sample MC-NH$_2$-1-a further decrease to 1,063 m^2/g, 0.7 cm^3/g and 2.3 and 4.8 nm, respectively. The degree of changes from this treatment is smaller than that in the oxidation. It implies that acylation-amidation is a milder step and amino groups have been successfully attached with carboxylic groups in the mesochannels. However, for the

ARTICLE

mesoporous carbon treated with prolonged oxidation time (16 h) and more EDA addition, both the surface area and pore volume (MC-NH$_2$-2-b) exhibit significant drops to just 520 m^2/g and 0.48 cm^3/g, respectively, which are ascribed to the damage on the mesostructure during the oxidation and partial

pore blockage by more amino groups modification. Thus, by controlling the conditions, an amino-functionalized mesoporous carbon with desired surface area, pore sizes and porosity can be obtained.

Table 1. Structural, textural parameters, nitrogen contents, surface charges and adsorption capacities of MC-LR for pristine and functionalized mesoporous carbon materials.

Sample	S_{BET} (m^2/g)	D (nm)	V_t (cm^3/g)	N (%)	Charged (pH 7)	Adsorbed MC-LR (mg/g)
MC	1680	2.8，5.5	1.67	0.21	negative	132
MC-COOH-1	1290	2.4，4.9	0.96	0.17	negative	69
MC-NH$_2$-1-a	1063	2.3，4.8	0.70	7.65	positive	159
MC-NH$_2$-2-b	520	1.9，5.2	0.48	10.96	positive	36

Surface Functionalities

Changes on the surface chemistry as a result of the chemical modifications are characterized by Fourier transform infrared (FTIR) spectroscopy (Figure 3). For the untreated mesoporous carbon, the weak band at around 1,628 cm^{-1} is ascribed to the vibration of C=C in the surface aromatic structures.[34] Another peak at 1,401 cm^{-1} is attributed to C-H bending vibration.[35] After the surface oxidation, new intense bands at 1,715 and 1,575 cm^{-1} appear for the carboxylic sample (MC-COOH). These bands can be attributed to the C=O of nonaromatic carboxyl groups and symmetric COO$^-$ vibration, implying the generation of many carboxylic functional groups.[25, 36] Another new band at 1,210 cm^{-1} can be assigned to the C-O bonds from phenolic, carboxylic and/or etheric groups, suggesting the generation of surface oxides. Meanwhile, the bond at 1,401 cm^{-1} of the untreated MC disappears, implying that the C-H groups are oxidized to C=O groups. For the following thionyl chloride treatment, the IR spectrum of the derivative MC-COCl shows a shifted peak of C=O stretching vibration from 1,715 to 1,728 cm^{-1} due to the negative inductive effect of chlorine atoms.[37] For the final product of amino-functionalized MC sample (MC-NH$_2$), a small band at 1,643 cm^{-1} appears and the band at a higher frequency of 1,715 cm^{-1} disappears, which can be assigned to the amide carbonyl C=O stretch instead of primary carboxylic ones.[38] The band around 1,540 cm^{-1} is ascribed to N-H plane stretch and one at 1,338 cm^{-1} is associated with C-N bond stretching, suggesting the presence of amine groups.[39, 40] In addition, the broad peaks between 1,000 – 1,250 cm^{-1} can be contributed to the vibration of C-N bond.[41] X-ray photoelectron spectroscopy (XPS) spectra are further used to analyze the functionalized mesoporous carbon materials in detail (SI Figure S4). The Cl 2p^3 spectrum of the derivative MC-COCl indicates that the acyl-chloride groups have generated onto the surface of carbon. For the amino-functionalized MC sample (MC-NH$_2$), the binding energies at around 399.8 and 401.5 eV on the N 1s spectrum correspond to the nitrogen in amide (-CONH-) and amine (-CNH2-) groups, respectively.[20, 37] Results clearly prove that the amino functional groups have been anchored to the carbon surface.

The C, H, and N compositions and corresponding densities of various functional groups of the pristine and treated MC samples are determined by elemental analysis. Results show sharply increased oxygen contents from 7.7 to ~ 36 wt. % and decreased carbon contents and small amount of hydrogen (~ 3%) after the first treatment of surface oxidation, implying the generation of oxygen-containing groups (SI Table S2). With longer duration of oxidation, more oxygen-containing groups are formed. After acylation and amidation for MC-COOH samples, the nitrogen contents increase greatly to 7.65 – 10.96 wt. % at different conditions with an increased hydrogen content and 10 wt. % decrease of oxygen, indicating that the nitrogen atoms have been incorporated onto the carbon surface. Amount of attached amines is estimated to 2.73, 3.43 and 3.84 mmol/g with various treated time and EDA addition. After the conversion, it reveals a high density of amino groups from 1.6 to 4.4 /nm^2.
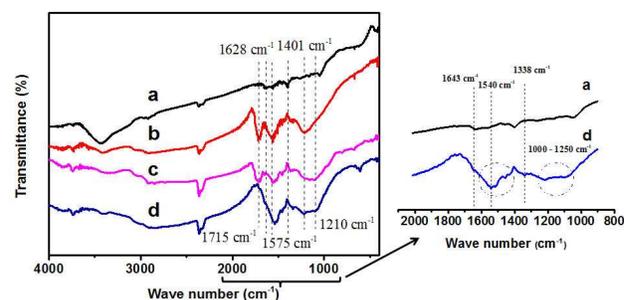
Fig. 3 FTIR spectra of pristine mesoporous carbon MC (a), MC-COOH sample treated with surface oxidation (b), MC-COCl sample further treated with thionyl chloride (c) and MC-NH$_2$ sample last treated by amidation (d). Partial magnification is on the right.

Thermogravimetric (TG) analyses further confirm the formation of various surface functional groups and their densities (SI Figure S5A). After the functionalization, the treated samples display weight losses. For the carboxylic mesoporous carbon (MC-COOH-1), weight loss of about 8 wt. % takes place at around 150 – 300°C, which can be contributed to the decomposition of the carboxylic groups.[25] The carboxyl group density is estimated at 2.5 mmol/g. When the amino

groups attach onto the materials (MC-NH$_2$-1-a), the weight loss (~ 8%) at the decomposition temperature of around 200 – 350°C is mainly attributed to the presence of the amino groups.[42] The densities of the functional groups can also be estimated from the weight loss data, which are comparable with the results from elemental analysis. The corresponding derivative thermogravimetric (DTG) plots of the pristine and functionalized mesoporous carbon materials demonstrate the different weight loss rates with the increased temperature (SI Figure S5B). The trends are similar to the profiles showed in the TG analyses.
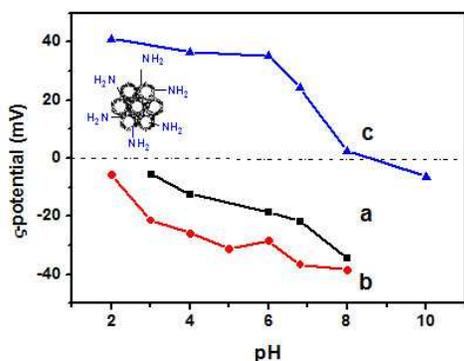
Fig. 4 Zeta potentials of pristine ordered mesoporous carbon MC (a), carboxyl functionalized MC-COOH (b) and amino functionalized MC-NH$_2$ mesoporous carbon (c) at different pH values.

Surface charges of the mesoporous carbon samples before and after each functionalization procedure are determined by Zeta-potential tests. The results (Figure 4) show that the isoelectric point (IEP) of the pristine mesoporous carbon MC is in the pH range of 2.0 ~ 3.0. In other words, the surface is negatively charged in the neutral pH range. After the surface acidic oxidation, the IEP is lower than 2.0 for the MC-COOH sample, because the formation of –COO$^-$ group leads to more negative charge on the surface of the mesoporous carbon. After grafting the amino group, the IEP of the MC-NH$_2$ to a higher pH value above 8. Such surface change from negative to positive charge at acidic and natural conditions is due to the deprotonization of –NH$_2$.[43]

Batch and Column Experiments on Microcystin-LR (MC-LR) Sorption

Four mesoporous carbon materials, including the pristine mesoporous carbon, a carboxyl modified MC-COOH and two amino modified MC-NH$_2$, are evaluated for batch adsorption of MC-LR to assess the impact of materials properties on the adsorption performance. All tests are for 4 hours as the adsorption equilibrium time according to the time-dependent adsorption curve (SI Figure S6). Under identical experimental conditions, MC-NH$_2$-1-a with the amino modification and high surface area shows the largest adsorption capacity of 159 mg/g, compared with 132 mg/g for the pristine mesoporous carbon, 69 mg/g for MC-COOH-1 and 36 mg/g for MC-NH$_2$-2-b. Furthermore, the adsorption isotherms of MC-LR on

mesoporous carbon and MC-NH$_2$-1-a are carried out to investigate the saturated adsorption behavior and capacity (Figure 5A). Two adsorption isotherms do not fit the Langmuir model with linear coefficient R^2 values of 0.948 and 0.947, respectively, implying that the adsorption of MC-LR on mesoporous carbon may incline to multi-layer adsorption (Figure 5B, C). Estimated from the Langmuir isotherms, the saturated adsorption capacity of amino-functionalized mesoporous carbon MC-NH$_2$-1-a is as high as 580 mg/g, larger than that for pristine mesoporous carbon (523 mg/g). Moreover, the adsorption ability is much higher than that (64 mg/g) of powder activated carbon (SI Figure S7 and Table S2). With pH in the range of 2 – 10, the adsorption capacity of MC-LR on sample MC-NH$_2$-1-a is determined (SI Figure S8). It shows a gradually decreased uptake with the increasing solution pH, suggesting a classical pH-dependent adsorption. The generation of more positive charges on the sorbent surface at lower pH promotes the affinity between sorbent and adsorbate MC-LR because of the stronger electrostatic attractions.
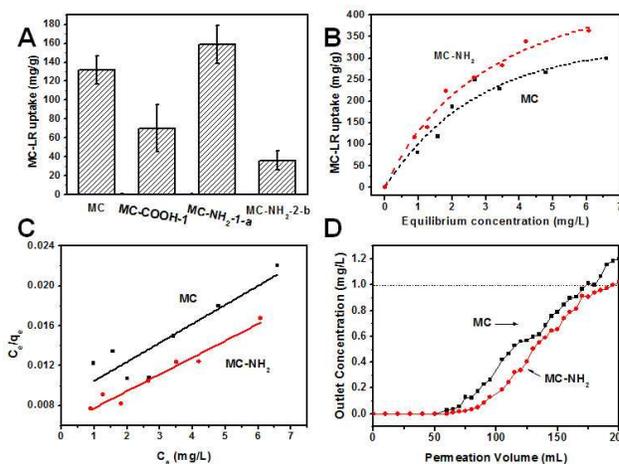
Fig. 5 Batch adsorption capacities of Microcystin-LR on different mesoporous carbon sorbents: (A) pristine MC, carboxyl modified MC-COOH-1, amino modified MC-NH$_2$-1-a and MC-NH$_2$-2-b with various amount of amino groups and surface areas, (B) adsorption isotherms, (C) the corresponding linear Langmuir modeling curves, and (D) column adsorption behaviors of two typical sorbents: the pristine mesoporous carbon MC and amino-modified mesoporous carbon MC-NH$_2$-1-a with high surface area.

The pristine and amino modified mesoporous carbons are further used as fillers in columns to test their adsorption behaviors of MC-LR (Figure 5D). The flowing streams pass through with a 10 mg/L of MC-LR solution at 25 mL/min (30 L/m^2 h). The breakthrough curve of the MC-LR solution reveals excellent adsorption behavior in the column with an undetected concentration at the outlet in the first stage (< 0.01 mg/L). The amino-functionalized sample MC-NH$_2$-1-a shows better adsorption property that the concentration of MC-LR solution is detected after a total volume of 55 mL feed solution passed through the column, comparing with 50 mL for pristine mesoporous carbon. After that, the concentration of effluent solution gradually increases. When the effluent concentration reaches 10% of the feed value, it is regarded as the breakthrough point of a column, which is often used to

calculate the adsorption capacity. According to this method, the adsorption capacity for MC-LR on the amino-functionalized mesoporous carbon MC-NH$_2$-1-a with high surface area in the column test is about 334 mg/g, compared to 305 mg/g on the pristine mesoporous carbon. Furthermore, when the adsorption ability of the sorbent descends or adsorption reaches saturation, regeneration of the spent sorbent is required. For the special sorbent MC-NH$_2$-1-a with high surface area, the adsorbed MC-LR molecules can be effectively eluted by methanol and then washed with water due to the high solubility of the MC-LR in methanol. Moreover, the methanol has no adverse influence on the structural and textural properties of sorbent and/or the chemical properties of functional groups –NH$_2$ for reuse. The amino-functionalized mesoporous carbon as a sorbent can be reused with less than 6% loss on the adsorption capacity after one recycle.

For the three modification procedures, surface oxidation is the most important step to achieve high surface area and density of amino groups. During this treatment, the carbon layers on the surface are removed gradually and partially dissolved while oxygen-containing groups are gradually generated and attached onto. If the degree of oxidation is insufficient, it leads to a low density of surface oxides and further affects the amount of amino groups. On the other hand, if the material is over-oxidized, the textural properties including surface areas and total pore volumes deteriorate significantly resulting in a low density of amino groups. In addition, it is also important for selection of the matrix. The unique mesoporous carbon is composed of bimodal mesopores with the secondary mesopores (2.8 nm) interpenetrating carbon walls and connecting primary mesopores (5.5 nm), which offers sufficient surfaces and spaces for subsequent fabrication of amino-functionalized mesoporous carbon with high surface area.

Of all the mesoporous carbon sorbents and powder activated carbon tested, the amino-modified mesoporous carbon MC-

NH$_2$-1-a shows the best adsorption performance for MC-LR removal. This can be explained from two perspectives (Scheme 1): firstly, it is the surface charge of the sorbent (Scheme 1B). Because the speciation of MC-LR with seven ionizable groups is highly pH sensitive, it has electronegative character in deionized water.[44] From the IEP measurements, surfaces of the pristine mesoporous carbon and the carboxyl modified MC-COOH are both negatively charged. When these materials are mixed with MC-LR, electrostatic repulsion drives the adsorbate away from sorbents. The carboxylic sample with more negative surface charge consequently results in much lower adsorption capacity (69 mg/g) than the pristine mesoporous carbon (132 mg/g). To the contrary, after the amino modification, the MC-NH$_2$-1-a sample is positively charged. Although its surface area and pore volume is somewhat lower, the electrostatic attractions from the opposite charges enhance adsorption capacity rapidly to 159 mg/g in batch adsorption and from 305 to 334 mg/g in the column adsorption. Secondly, the structural and textural property of the sorbent is also important to affect the adsorption capacity (Scheme 1A). The surface area and pore volume of the sample MC-NH$_2$-1-a decreases by 33% compared to the original mesoporous carbon, but still maintain relatively high values of 1,063 m^2/g and 0.7 cm^3/g with plenty of adsorption sites and spaces. For the sample MC-NH$_2$-2-b, because of the long oxidation time, the surface area drops by as much as 67%, there is a serious damage on the pore channels which lows the number of adsorption sites. As a result, although the density of the attached amino groups is high, it shows the lowest adsorption performance for MC-LR (36 mg/g). For easy comparison between the pristine and the amino-functionalized carbon MC-NH$_2$-1-a, their adsorption capacities are normalized to the unit area (adsorption capacity divided by the surface area). Results show that the amino group modification nearly doubles the adsorption ability.
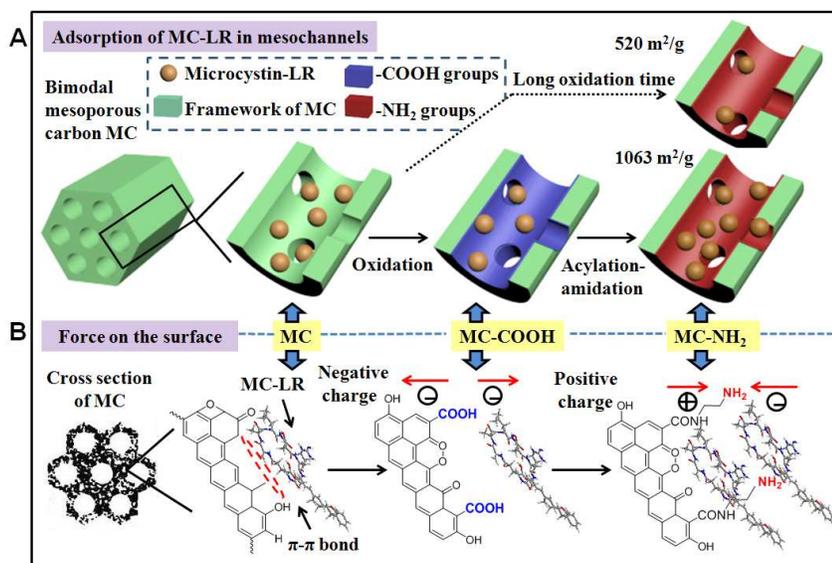
Scheme 1 Adsorption mechanisms of microcystins-LR in mesopore channels (A) and acting forces on the surface (B) on pristine mesoporous carbon MC, carboxyl-functionalized MC-COOH and amino-functionalized MC-NH$_2$ with different surface areas.

Journal of Materials Chemistry A

ARTICLE

Conclusions

Amino-functionalized ordered mesoporous carbon possessing high surface area (1063 m^2/g) and large pore volume (0.7 cm^3/g) has been synthesized by a three-step chemical modification, based on a bimodal mesoporous carbon (2.3 and 5.9 nm) matrix. The carboxyl groups first are generated on the carbon surface through wet oxidation, and then, by acylation-amidation with SOCl$_2$ and EDA to couple with amino groups on. The ordered mesostructures and good textural properties of the functionalized mesoporous carbons can be adjusted by the surface oxidation time and the addition of EDA in amidation. The treatment of surface oxidation plays a vital role in the finally exceptional structural and chemical properties. High-density amino groups can be introduced (up to ~ 3.84 mmol/g), and make a change from negative to positive charges on the surface, with the isoelectric point of the mesoporous carbon adsorbent shifting from 2 to 8. Due to the synergy with high density of amino-functional groups, high surface area and interconnected large mesopores, the adsorbent MC-NH$_2$-1-a demonstrates the best adsorption performances (580 and 334 mg/L for batch and column adsorption respectively) to remove the toxic MC-LR from water, capable of doubling the adsorption capacity in a unit surface area compared with the pristine mesoporous carbon. It also exhibits rapid adsorption behaviors on the column tests along with stable cyclic performances for regeneration. Such amino functionalized mesoporous carbon can be utilized for wider applications, such as the removal of acidic or positively charged contaminants with large molecular sizes from waster water or CO$_2$ in the contaminated air, or as a support for further immobilization and functionalization for drug delivery and catalysis.

Acknowledgements

Notes and references

1 Y. Wan, Y. F. Shi and D. Y. Zhao, *Chem. Commun.*, 2008, **20**, 932-945.

2 R. Liu, Y. Shi, Y. Wan, Y. Meng, F. Zhang, D. Gu, Z. Chen, B. Tu and D. Zhao, *J. Am. Chem. Soc.*, 2006, **128**, 11652-11662.

3 J. Zhu, H. Gu, J. Guo, M. Chen, H. Wei, Z. Luo, H. A. Colorado, N. Yerra, D. Ding, T. C. Ho, N. Haldolaarachchige, J. Hopper, D. P. Young, Z. Guo and S. Wei, *J Mater. Chem. A*, 2014, **2**, 2256-2265.

4 B. Qiu, Y. Wang, D. Sun, Q. Wang, X. Zhang, B. L. Weeks, R. O'Connor, X. Huang, S. Wei and Z. Guo, *J. Mater. Chem. A*, 2015, **3**, 9817-9825.

5 F. Q. Zhang, Y. Meng, D. Gu, Y. Yan, C. Z. Yu, B. Tu and D. Y. Zhao, *J. Am. Chem. Soc.*, 2005, **127**, 13508-13509.

6 C. F. Xue, B. Tu and D. Y. Zhao, *Nano Res.*, 2009, **2**, 242-253.

7 C. D. Liang, Z. J. Li and S. Dai, *Angew. Chem. Int. Edit.*, 2008, **47**, 3696-3717.

8 A. Stein, Z. Y. Wang and M. A. Fierke, *Adv. Mater.*, 2009, **21**, 265-293.

9 B. Qiu, C. Xu, D. Sun, H. Wei, X. Zhang, J. Guo, Q. Wang, D. Rutman, Z. Guo and S. Wei, *RSC Adv.*, 2014, **4**, 29855-29865.

10 P. Chingombe, B. Saha and R. J. Wakeman, *Carbon*, 2005, **43**, 3132-3143.

11 M. Choi and R. Ryoo, *J. Mater. Chem.*, 2007, **17**, 4204-4209.

12 L. F. Wang, Y. Zhao, K. F. Lin, X. J. Zhao, Z. C. Shan, Y. Di, Z. H. Sun, X. J. Cao, Y. C. Zou, D. Z. Jiang, L. Jiang and F. S. Xiao, *Carbon*, 2006, **44**, 1336-1339.

13 V. L. Budarin, J. H. Clark, R. Luque and D. J. Macquarrie, *Chem. Commun.*, 2007, 634-636.

14 T. Chen, T. Wang, D. J. Wang, J. Q. Zhao, X. C. Ding, S. C. Wu, H. R. Xue and J. P. He, *Acta Phys.-Chim. Sin.*, 2010, **26**, 3249-3256.

15 B. Qiu, C. Xu, D. Sun, H. Yi, J. Guo, X. Zhang, H. Qu, M. Guerrero, X. Wang, N. Noel, Z. Luo, Z. Guo and S. Wei, *ACS Sustain. Chem. Eng.*, 2014, **2**, 2070-2080.

16 J. L. Figueiredo, M. Pereira, M. Freitas and J. Orfao, *Carbon*, 1999, **37**, 1379-1389.

17 S. Murugesan, K. Myers and V. Subramanian, *Appl. catal. B-environ.*, 2011, **103**, 266-274.

18 T. Ramanathan, F. T. Fisher, R. S. Ruoff and L. C. Brinson, *Chem. Mater.*, 2005, **17**, 1290-1295.

19 A. Villa, J. Tessonnier, O. Majoulet, D. S. Su and R. Schlogl, *Chem. Commun.*, 2009, 4405-4407.

20 C. Yuan, W. Chen and L. Yan, *J. Mater. Chem.*, 2012, **22**, 7456-7460.

21 Y. Hu, J. Shen, N. Li, M. Shi, H. Ma, B. Yan, W. Wang, W. Huang and M. Ye, *Polym. Composite.*, 2010, **31**, 1987-1994.

22 S. K. Singh, M. K. Singh, P. P. Kulkarni, V. K. Sonkar, J. Gracio and D. Dash, *ACS Nano*, 2012, **6**, 2731-2740.

23 A. Vinu, K. Z. Hossian, P. Srinivasu, M. Miyahara, S. Anandan, N. Gokulakrishnan, T. Mori, K. Ariga and V. V. Balasubramanian, *J. Mater. Chem.*, 2007, **17**, 1819-1825.

Journal of Materials Chemistry A Accepted Manuscript

24 P. Srinivasu, V. V. Balasubramanian, L. Kumaresan, D. P. Sawant, X. Jin, S. Alam, K. Ariga, T. Mori and A. Vinu, *J. Nanosci. Nanotechno.*, 2007, **7**, 3250-3256.

25 Z. X. Wu, P. A. Webley and D. Y. Zhao, *Langmuir*, 2010, **26**, 10277-10286.

26 C. Svrcek and D. W. Smith, *Environ. Sci. Technol.*, 2004, **3**, 155-185.

27 V. M. Vasconcelos, K. Sivonen, W. R. Evans, W. W. Carmichael and M. Namikoshi, *Water Res.*, 1996, **30**, 2377-2384.

28 W. Song, A. A. de la Cruz, K. Rein and K. E. O'Shea, *Environ. Sci. Technol.*, 2006, **40**, 3941-3946.

29 X. Wu, B. Xiao, R. Li, C. Wang, J. Huang and Z. Wang, *Environ. Sci. Technol.*, 2011, **45**, 2641-2647.

30 R. M. Dawson, *Toxicon*, 1998, **36**, 953-962.

31 T. Lanaras, C. M. Cook, J. E. Eriksson, J. A. O. Meriluoto and M. Hotokka, *Toxicon*, 1991, **29**, 901-906.

32 W. Teng, Z. X. Wu, J. W. Fan, H. Chen, D. Feng, Y. Y. Lv, J. X. Wang, A. M. Asiri and D. Y. Zhao, *Energy Environ. Sci.*, 2013, **6**, 2765-2776.

33 W. Teng, Z. X. Wu, D. Feng, J. W. Fan, J. X. Wang, H. Wei, M. J. Song and D. Y. Zhao, *Environ. Sci. Technol.*, 2013, **47**, 8633-8641.

34 Y. F. Jia and K. M. Thomas, *Langmuir*, 2000, **16**, 1114-1122.

35 C. Moreno-Castilla, M. V. Lopez-Ramon and F. Carrasco-Marin, *Carbon*, 2000, **38**, 1995-2001.

36 J. W. Shim, S. J. Park and S. K. Ryu, *Carbon*, 2001, **39**, 1635-1642.

37 J. Shen, W. Huang, L. Wu, Y. Hu and M. Ye, *Compos. Part A-Appl. S.*, 2007, **38**, 1331-1336.

38 G. Vuković, A. Marinković, M. Obradović, V. Radmilović, M. Čolić, R. Aleksić and P. S. Uskoković, *Appl. Surf. Sci.,* 2009, **255**, 8067-8075.

39 K. Awasthi, D. P. Singh, S. Singh, D. Dash and O. N. Srivastava, *New Carbon Mater.*, 2009, **24**, 301-306.

40 T. Ramanathan, F. T. Fisher, R. S. Ruoff and L. C. Brinson, *Chem. Mater.*, 2005, **17**, 1290-1295.

41 E. Salehi, S. S. Madaeni, L. Rajabi, V. Vatanpour, A. A. Derakhshan, S. Zinadini, S. Ghorabi and H. Ahmadi Monfared, *Sep. Purif. Technol.*, 2012, **89**, 309-319.

42 S. Murugesan, K. Myers and V. R. Subramanian, *Appl. Catal. B-Environ.*, 2011, **103**, 266-274.

43 J. M. Rosenholm and M. Linden, *Chem. Mater.*, 2007, **19**, 5023-5034.

44 P. De Maagd, A. J. Hendriks, W. Seinen and D. Sijm, *Water Res.*, 1999, **33**, 677-680.

Graphical and Textual

Amino-functionalized ordered mesoporous carbons were prepared with a high surface area and high-density amino groups, exhibiting preeminent static and dynamic adsorption capabilities (580 and 334 mg/g respectively) for Microcystin-LR removal.